

PPR: Enhancing Dodging Attacks while Maintaining Impersonation Attacks on Face Recognition Systems

Fengfan Zhou¹ Hefei Ling¹ Bangjie Yin² Hui Zheng²

Abstract

Adversarial Attacks on Face Recognition (FR) encompass two types: impersonation attacks and evasion attacks. We observe that achieving a successful impersonation attack on FR does not necessarily ensure a successful dodging attack on FR in the black-box setting. Introducing a novel attack method named **P**re-training **P**runing **R**estoration Attack (PPR), we aim to enhance the performance of dodging attacks whilst avoiding the degradation of impersonation attacks. Our method employs adversarial example pruning, enabling a portion of adversarial perturbations to be set to zero, while tending to maintain the attack performance. By utilizing adversarial example pruning, we can prune the pre-trained adversarial examples and selectively free up certain adversarial perturbations. Thereafter, we embed adversarial perturbations in the pruned area, which enhances the dodging performance of the adversarial face examples. The effectiveness of our proposed attack method is demonstrated through our experimental results, showcasing its superior performance.

1. Introduction

Thanks to the ceaseless advancements in deep learning, FR has made remarkable strides in achieving exceptional levels of performance(Schroff et al., 2015)(Wang et al., 2018)(Deng et al., 2022). However, the vulnerability of existing FR models to adversarial attacks poses a significant threat to their security.

Hence, there is an urgent need to enhance the performance of adversarial face examples to expose more blind spots in

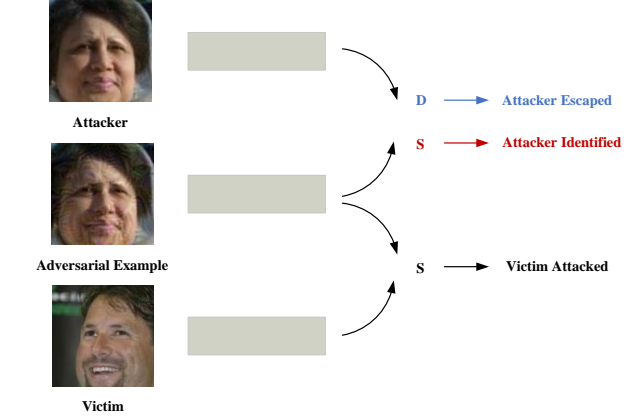


Figure 1. An example of comparison between our proposed attack (blue) and the traditional impersonation attack (red) in the black-box setting. The letters ‘D’ and ‘S’ signify that the FR model classifies the two face images as belonging to different identities and belonging to the same identity, respectively.

FR models. Consequently, several research endeavors have been directed towards this realm.

A multitude of adversarial attacks have been developed to create adversarial face examples with characteristics such as stealthiness(Qiu et al., 2020)(Yang et al., 2021)(Cherepanova et al., 2021)(Hu et al., 2022)(Shamshad et al., 2023), transferability(Zhong & Deng, 2021)(Zhou et al., 2023b)(Zhou et al., 2023a), and physical attack capability(Yin et al., 2021)(Yang et al., 2023)(Li et al., 2023b). These efforts contribute to enhancing the effectiveness of existing attacks using face adversarial examples. However, these studies primarily concentrate on bolstering either impersonation attacks or dodging attacks, overlooking the exploration of the effectiveness of dodging attacks when crafting adversarial face examples using the impersonation attacks.

Unlike image classification, FR is an open-set task. Predicting the class probability of identities in real-world deployment is an extremely challenging task. In practical FR applications, we extract embeddings from two face images using the FR model. Subsequently, the distance between the

Preprint. ¹Huazhong University of Science and Technology
²Shanghai Shizhuang Information Technology Co., Ltd. Correspondence to: Hefei Ling <lhefei@hust.edu.cn>.

Proceedings of the 41st International Conference on Machine Learning, Vienna, Austria. PMLR 235, 2024. Copyright 2024 by the author(s).

two embeddings is used to determine whether the images belong to the same identity. If the distance falls below a predefined threshold, the two images are recognized as belonging to the same identity; otherwise, they are classified as different identities. Based the measurement of FR, there exists the samples that can be classified as two different identities in theory. We denote these samples as *multi-identity samples*. Our experiments have verified the existence of multi-identity samples on common-used face dataset (refer to Appendix A).

In impersonation attacks, the objective is to deceive the FR model into recognizing adversarial face examples as a pre-defined identity, which requires that the distance between the embeddings of the adversarial face example and the victim image be lower than the threshold. On the other hand, in dodging attacks, the aim is to trick the FR model into recognizing the adversarial face example as identities other than the attacker, which means that the distance between the embeddings of the adversarial face example and the attacker image should be greater than the threshold. The existence of multi-identity samples implies that a successful impersonation attack on FR does not necessarily guarantee a successful dodging attack on FR in theory. Our experiment confirms that the majority of adversarial face examples crafted by traditional impersonation attacks, which can successfully perform impersonation attacks, fail to perform dodging attacks in the black-box setting (see Appendix B).

In practical application scenarios, criminals tend to generate adversarial examples with their own faces to deceive FR models into recognizing them as victims for impersonation attacks, while avoiding being recognized as criminals themselves for dodging attacks to escape legal prosecution. This necessitates the generation of adversarial examples that can perform both impersonation and dodging attacks.

To improve the dodging performance of the adversarial face examples without degrading the impersonation performance, we propose a novel attack method, termed as **Pre-training Pruning Restoration Attack (PPR)**. Specifically, inspired by the pruning methods in model compression, we prune the pre-trained adversarial face examples to sparsify the adversarial face examples. Subsequently, we add adversarial perturbations that favor dodging attacks on the pruned regions to improve the dodging performance of the adversarial face examples (i.e. the operation of *Restoration*). After pruning and restoration, the impersonation performance of the adversarial face examples can be maintained and the dodging performance of the adversarial face examples can be improved.

Figure 1 illustrates a comparison between our proposed attack and the traditional impersonation attack. The adversarial face example generated by our proposed attack method successfully evades identification as the attacker in

contrast with the adversarial face example crafted by the traditional impersonation attack method is identified as the attacker. The adversarial face example generated by our proposed attack method successfully evades identification as the attacker, while the adversarial face example crafted by the traditional impersonation attack method is identified as the attacker. Note that both the adversarial face examples crafted by our proposed attack method and the traditional impersonation attack method are capable of being identified as the victim image.

Our main contributions are summarized as follows:

- We verify the universality of multi-identity samples among adversarial face examples crafted by traditional impersonation attacks and demonstrate that a successful impersonation attack does not necessarily equate to a successful dodging attack on FR systems.
- We propose a novel adversarial attack method called PPR based on adversarial example pruning. By pruning the adversarial face examples and subsequently introducing adversarial perturbations favoring dodging attacks, we effectively enhance the dodging performance. The approach allows us to maintain the impersonation performance while significantly improving the dodging performance of the adversarial face examples.
- Extensive experiments demonstrate that our proposed method achieves superior performance compared to the baseline adversarial attack methods.

2. Related Works

2.1. Adversarial Attacks

The primary objective of adversarial attacks is to introduce imperceptible perturbations to benign images for the purpose of deceiving machine learning systems and causing them to make mistakes(Szegedy et al., 2014)(Goodfellow et al., 2015). The existence of adversarial examples poses a significant threat to the security of current machine learning systems. Lots of efforts have been dedicated to researching adversarial attacks in order to enhance the robustness of these systems(Long et al., 2022)(Zhang et al., 2022)(Liang et al., 2023)(Wei et al., 2023)(Lu et al., 2023).

To improve the performance of black-box adversarial attacks, DI is proposed by (Xie et al., 2019) to randomly transform adversarial examples in each iteration. VMI-FGSM, proposed by (Wang & He, 2021), employs gradient variance to stabilize the updating process of adversarial examples, boosting the black-box performance. SSA, as proposed by (Long et al., 2022), transforms adversarial examples into the frequency domain and uses spectrum transformation to augment them. (Wang et al., 2023b) propose SIA.

SIA applies a random image transformation to each image block, generating a varied collection of images that are then employed for gradient calculations. (Wang et al., 2023a) propose BSR. BSR divides the input image into multiple blocks, subsequently shuffling and rotating these blocks in a random manner, creating a collection of new images for the purpose of gradient calculation.

2.2. Face Recognition

FR is an open-set task, meaning we cannot predict the class of a user upon deploying an FR model. As a result, relying solely on the maximum probability value of the output of the neural network to determine the class the of a user becomes impractical. Instead, when deploying the FR model, we extract the embeddings of two images and compute the similarity between them. If the similarity exceeds a predefined threshold, we conclude that the two images belong to the same identity; otherwise, they belong to different identities.

Recent research on FR primarily focuses on reducing the intra-class distance and increasing the inter-class distance of embeddings extracted by FR models. (Schroff et al., 2015) introduce FaceNet that employs triplet loss to map face images into a space where the distance represents the dissimilarity between them. (Wang et al., 2018) develop CosFace, which utilizes the large-margin cosine loss to enhance FR model performance. Additionally, (Deng et al., 2022) introduce ArcFace that incorporates the additive angular margin loss to train FR models that extract more discriminative features.

2.3. Adversarial Attacks on Face Recognition

Adversarial attacks on FR can be mainly classified into two categories: restricted attacks and unrestricted attacks.

Restricted attacks on FR are the attacks that generate adversarial examples in a restricted bound (e.g. L_p bound). Because FR belongs to the open-set task, the embedding-level loss is more suitable. Therefore, (Zhong & Deng, 2019) proposed FIM that use embedding-level loss to craft the adversarial face examples. (Zhong & Deng, 2021) proposed DFANet that performs dropout on the feature maps of the convolutional layers to improve the transferability. (Yang et al., 2021) propose TIP-IM to improve the face encryption. TIP-IM use MMD(Borgwardt et al., 2006) loss to improve the quality of encrypted face images and use the greedy insertion to select the optimal victim images. (Zhou et al., 2023b) propose BPFA to improve the transferability of adversarial attacks on FR by adding beneficial perturbations(Wen & Itti) on the features maps of the FR models to obtain effect that is similar to hard samples augmentation.

The unrestricted adversarial attacks on FR are the attacks that generate adversarial examples without the restriction of

a predefined bound. The unrestricted adversarial attacks on FR mainly focus on physical attacks(Xiao et al., 2021)(Yang et al., 2023)(Li et al., 2023a), attribute editing(Jia et al., 2022) and generating adversarial examples based on makeup transfer(Yin et al., 2021)(Hu et al., 2022)(Shamshad et al., 2023).

3. Methodology

3.1. Problem Formulation

In the context of our study, $\mathcal{F}^{vct}(x)$ denotes the FR model used by the victim to extract the embedding from a face image x . We refer to x^s and x^t as the attacker and victim images, respectively. The objective of the impersonation attacks explored in our research is to manipulate \mathcal{F}^{vct} into misclassifying x^{adv} as x^t , while ensuring that x^{adv} bears a close visual resemblance to x^s . To be more specific, the objective can be expressed as follows:

$$\begin{aligned} x^{adv} = \arg \min_{x^{adv}} & (\mathcal{D}(\mathcal{F}^{vct}(x^{adv}), \mathcal{F}^{vct}(x^t))) \\ \text{s.t.} & \|x^{adv} - x^s\|_p \leq \epsilon \end{aligned} \quad (1)$$

where \mathcal{D} refers to a predefined distance metric, while ϵ specifies the maximum magnitude of permissible perturbation. By contrast, the objective of the dodging attacks proposed in this study is to render $\mathcal{F}^{vct}(x)$ unable to identify x^{adv} as x^s , while simultaneously ensuring that x^{adv} bears a visual resemblance to x^s . In a manner similar to impersonation attacks, the objective of dodging attacks can be formulated as follows:

$$\begin{aligned} x^{adv} = \arg \max_{x^{adv}} & (\mathcal{D}(\mathcal{F}^{vct}(x^{adv}), \mathcal{F}^{vct}(x^s))) \\ \text{s.t.} & \|x^{adv} - x^s\|_p \leq \epsilon \end{aligned} \quad (2)$$

Due to the differing objectives of the impersonation and dodging attacks, the calculation methods for the ASR also vary between the two attack types. When it comes to impersonation attacks on FR, the ASR can be computed as:

$$\text{ASR}^i = \frac{\sum_{i=1}^{N_p} \mathbb{1}(\mathcal{D}(\mathcal{F}^{vct}(x^{adv}), \mathcal{F}^{vct}(x^t)) < t^i)}{N_p} \quad (3)$$

where N_p refers to the total number of face pairs and t^i represents the impersonation attack threshold. For dodging attacks on FR systems, the ASR can be computed via the following formula:

$$\text{ASR}^d = \frac{\sum_{i=1}^{N_p} \mathbb{1}(\mathcal{D}(\mathcal{F}^{vct}(x^{adv}), \mathcal{F}^{vct}(x^s)) > t^d)}{N_p} \quad (4)$$

where the value of t^d represents the threshold for dodging attacks.

3.2. Exploring the Impersonation and Dodging Attack on Face Recognition

In most cases, the victim model \mathcal{F}^{vct} is not accessible to the attacker, making it impossible to optimize objectives as stated in Equation (1) and Equation (2) directly. To circumvent this issue, a common approach is to leverage a surrogate model \mathcal{F} accessible to the attacker to generate adversaries that can be transferred to the victim model for an effective attack(Yuan et al., 2022)(Zhang et al., 2022)(Naseer et al., 2023)(Wang et al., 2023b)(Wang et al., 2023a).

For impersonation attacks, the loss can be formulated as follows:

$$\mathcal{L}^i = \|\phi(\mathcal{F}(x^{adv})) - \phi(\mathcal{F}(x^t))\|_2^2 \quad (5)$$

where $\phi(x)$ represents the operation that normalizes x . x^{adv} is the adversarial example which is initialized with the same value as x^s . Dodging attacks can be formulated with the following loss function:

$$\mathcal{L}^d = -\|\phi(\mathcal{F}(x^{adv})) - \phi(\mathcal{F}(x^s))\|_2^2 \quad (6)$$

As the FR task is an open-set task, it is not possible to predict the classes of users during the practical deployment of the FR model. Therefore, we need to compare the similarity between two face images in order to discern whether they depict the same identity or not. Based on the identification method in face recognition, multi-identity samples exist theoretically. Our experiments verify the existence of such samples among benign face images. The existence of multi-identity samples raises a question:

Does the success of an impersonation attack imply the success of dodging attack on FR systems?

To this end, we generated face adversarial samples using the traditional impersonation attack and evaluate its dodging ASR (refer to Appendix B). Our experiments demonstrate that the majority of adversarial face examples crafted by traditional impersonation attack cannot achieve a successful dodging attack in the black-box setting.

Nonetheless, in real-world adversarial attacks, attackers do not want the adversarial face examples to be recognized as themselves, as this could lead to legal consequences. Hence, it is crucial to research attack techniques that can execute both impersonation and dodging attacks simultaneously. Traditional impersonation attacks on FR systems have shown a remarkably high level of impersonation ASR in black-box settings. Therefore, our objective is to enhance the dodging performance while maintaining the impersonation effectiveness of traditional impersonation attacks.

To accomplish this objective, a straightforward approach is to generate adversarial face examples by employing a

Lagrangian attack strategy that utilizes the following loss function:

$$\mathcal{L} = \lambda \mathcal{L}^i + \mathcal{L}^d \quad (7)$$

However, due to the conflict between the optimization between \mathcal{L}^i and \mathcal{L}^d , there exists a trade-off between the performance of impersonation and dodging performance leading to subpar performance (See Section 4.2). If we alleviate the trade-off, we can achieve a better dodging performance while maintaining the impersonation performance.

3.3. Pre-training Pruning Restoration Attack

To accomplish this objective, a straightforward approach is to fine-tune the adversarial face examples generated by the Lagrangian attack with a lower λ value in order to enhance the performance of dodging attacks. However, this method does not enhance the dodging attack performance without compromising the impersonation attack performance (see *Fine-tuning* in Table 4). We contend that this issue arises because the newly introduced adversarial perturbation that favors dodging attacks ends up disrupting the pre-existing adversarial perturbation patterns. While it may improve the performance of dodging attacks, it inevitably diminishes the performance of impersonation attacks. To address this, we introduce new adversarial perturbations favoring dodging attacks in regions where the original perturbations have not been added. However, identifying suitable areas for these new perturbations is challenging due to their scarcity. Therefore, drawing inspiration from prior works in model pruning(Ma et al., 2023)(Frantar & Alistarh, 2023), we propose incorporating pruning into the realm of adversarial face examples. The aim is to free up some model parameters while minimizing the decrease in the performance of impersonation attacks, thereby creating space to introduce perturbations that facilitate dodging attacks.

In order to prune the adversarial perturbation, our initial step is to assess its importance by identifying and sparsifying the less important regions. To estimate this importance, we propose utilizing the magnitude of the adversarial perturbation as a measure. A lower magnitude implies a lesser impact on the performance of the adversarial examples generated after sparsification.

Let the adversarial examples be x^{adv} . The formula to calculate the importance can be express as:

$$\mathcal{I} = |x^{adv} - x^s| \quad (8)$$

where $\mathcal{I} \in \mathbb{R}^{CHW}$. C, H, and W are the channel number, height, width of the face images, respectively.

Let κ be the sparsity ratio for pruning the adversarial face examples that measures the ratio of adversarial perturbations to be set into zero. Let s be the number of adversarial

perturbation elements:

$$s = \text{CHW} \quad (9)$$

We arrange the elements in flattened vector of \mathcal{I} in ascending order (from the lowest to the highest):

$$\mathcal{Q} = \text{Sort}(\Psi(\mathcal{I})) \quad (10)$$

where Ψ is the flatten operation.

Let \mathcal{W} be the set of the elements of the adversarial perturbations to be pruned. Given the importance calculation method for pruning, the value of \mathcal{W} can be calculated as follows:

$$\mathcal{W} = \mathcal{Q}[:, \kappa s] \quad (11)$$

where the colon denotes the slice operation to obtain the first κs elements.

The mask for pruning can be obtained using \mathcal{W} :

$$\mathcal{M}_{i,j,k} = \begin{cases} 0, & \text{if } \mathcal{I}_{i,j,k} \in \mathcal{W} \\ 1, & \text{if } \mathcal{I}_{i,j,k} \notin \mathcal{W} \end{cases} \quad (12)$$

By utilizing the mask, we can apply the following formula to prune the adversarial example:

$$\bar{x}^{adv} = x^s + (x^{adv} - x^s) \odot \mathcal{M} \quad (13)$$

Once the adversarial face examples are pruned, we can proceed to restore the adversarial perturbations in the pruned regions. The mask representing the regions for restoring the adversarial examples can be denoted as:

$$\mathcal{A} = 1 - \mathcal{M} \quad (14)$$

For both the pre-training and restoration stages, various adversarial attacks can be employed. In the following, we will illustrate the pre-training and restoration stages of our proposed method by using the Lagrangian attack as an example. In the stage of pre-training, we utilize Equation (7) as the pre-training loss \mathcal{L}^p to craft the adversarial face examples:

$$x_t^{adv} = x_{t-1}^{adv} - \beta \text{sign}(\nabla_{x_{t-1}^{adv}} \mathcal{L}^p) \quad (15)$$

where t is the iteration of optimization process of adversarial examples, β is the step size when optimizing the adversarial face examples in the pre-training stage.

Once the adversarial examples are pre-trained, we utilize our proposed method of pruning adversarial face examples to free up some adversarial perturbations. During the restoration stage, we restore the adversarial face examples in the previously pruned region using the following loss function:

$$\mathcal{L}^r = \tilde{\lambda} \mathcal{L}^i + \mathcal{L}^d \quad (16)$$

where $\tilde{\lambda}$ is a weight which is lower than λ that is objective for crafting adversarial face examples that favor dodging attacks.

$$x_t^{adv} = x_{t-1}^{adv} - \gamma \text{sign}(\nabla_{x_{t-1}^{adv}} \mathcal{L}^r) \quad (17)$$

where γ is the step size when optimizing the adversarial face examples in the restoration stage. The algorithm of our proposed method based on Lagrangian attack are illustrated in Algorithm 1.

Algorithm 1 Pre-training Pruning Restoration Attack Based on Lagrangian

Input: Negative face image pair $\{x^s, x^t\}$, the step size of the adversarial perturbations β , the number of the iterations of pre-training stage n , the maximum number of iterations m , maximum allowable perturbation magnitude ϵ , the surrogate FR model \mathcal{F} .

Output: An adversarial face example x_m^{adv}

1: $x_0^{adv} = x^s$
 2: **for** $t = 1, \dots, n$ **do** ▷ Pre-training Stage
 3: $\mathcal{L}^p = \lambda \mathcal{L}^i + \mathcal{L}^d$
 4: $x_t^{adv} = x_{t-1}^{adv} - \beta \text{sign}(\nabla_{x_{t-1}^{adv}} \mathcal{L}^p)$
 5: $x_t^{adv} = \prod_{x^s, \epsilon} (x_t^{adv})$
 6: **end for** ▷ Pruning Stage
 7: $\mathcal{I} = |x_n^{adv} - x^s|$
 8: $\mathcal{Q} = \text{Sort}(\Psi(\mathcal{I}))$
 9: $\mathcal{W} = \mathcal{Q}[:, \kappa s]$
 10: Get \mathcal{M} by Equation (12).
 11: $x_n^{adv} = x^s + (x_n^{adv} - x^s) \odot \mathcal{M}$
 12: $\mathcal{A} = 1 - \mathcal{M}$
 13: **for** $t = n + 1, \dots, m$ **do** ▷ Restoration Stage
 14: $\mathcal{L}^r = \tilde{\lambda} \mathcal{L}^i + \mathcal{L}^d$
 15: $x_t^{adv} = x_{t-1}^{adv} - \gamma \text{sign}(\nabla_{x_{t-1}^{adv}} \mathcal{L}^r)$
 16: $p = \mathcal{A} \odot (x_t^{adv} - x_n^{adv})$
 17: $x_t^{adv} = \prod_{x^s, \epsilon} (x_n^{adv} + p)$
 18: **end for**

4. Experiments

4.1. Experimental Setting

Datasets. We have opted to use the LFW dataset (Huang et al., 2007) and the CelebA-HQ dataset (Karras et al., 2018) for our experiments. LFW serves as an unconstrained face dataset for FR, while CelebA-HQ consists of high-quality images. These two datasets are widely employed in research on adversarial attacks in FR (Xiao et al., 2021; Yin et al., 2021; Hu et al., 2022). The LFW and CelebA-HQ datasets utilized in our experiments are identical to those employed in previous studies (Zhou et al., 2023b;a).

Table 1. Comparisons of dodging ASR results for attacks on the LFW and CelebA-HQ datasets. The surrogate models are presented in the first column, and the victim models are listed in the second row.

Surrogate Model	Attack	LFW			CelebA-HQ		
		IR152	FaceNet	MF	IR152	FaceNet	MF
IR152	DI	95.4 / 100.0	5.8 / 11.3	0.2 / 0.8	87.9 / 100.0	8.4 / 16.4	0.4 / 1.2
	VMI	92.7 / 100.0	17.3 / 32.5	1.2 / 9.5	92.2 / 100.0	14.3 / 27.9	1.2 / 4.1
	SSA	78.8 / 100.0	5.7 / 22.5	0.9 / 10.6	83.8 / 99.9	7.2 / 19.6	0.4 / 5.6
	DFANet	98.9 / 100.0	1.4 / 4.2	0.0 / 0.3	98.9 / 100.0	2.3 / 6.0	0.0 / 0.4
	SIA	81.7 / 100.0	13.0 / 37.5	0.8 / 8.9	78.4 / 100.0	13.2 / 35.6	0.7 / 7.4
	BSR	52.4 / 100.0	5.3 / 17.6	0.1 / 1.5	48.5 / 99.9	5.4 / 18.0	0.3 / 1.9
	BPFA	92.6 / 100.0	1.7 / 7.3	0.0 / 1.2	90.4 / 100.0	2.1 / 8.1	0.1 / 0.8
FaceNet	DI	5.3 / 10.3	99.8 / 99.9	3.1 / 10.3	1.5 / 3.1	99.4 / 99.9	1.8 / 4.7
	VMI	9.7 / 14.3	99.8 / 99.9	6.2 / 13.2	3.1 / 7.1	99.3 / 99.8	3.6 / 9.3
	SSA	6.0 / 14.0	97.5 / 99.9	6.6 / 26.2	2.0 / 5.5	96.9 / 99.7	4.2 / 14.6
	DFANet	1.6 / 3.3	99.8 / 99.9	0.4 / 2.7	0.5 / 2.6	99.1 / 100.0	0.8 / 4.1
	SIA	11.2 / 20.6	99.5 / 99.9	8.7 / 21.2	4.0 / 8.9	99.4 / 99.9	5.4 / 13.7
	BSR	12.2 / 19.2	98.6 / 99.9	9.0 / 17.8	4.6 / 10.1	98.8 / 99.9	5.3 / 14.1
	BPFA	4.7 / 16.8	98.6 / 100.0	1.6 / 15.0	1.1 / 4.2	99.0 / 100.0	0.6 / 5.1
MF	DI	2.2 / 7.3	18.2 / 36.4	99.2 / 100.0	0.1 / 2.5	12.1 / 31.3	95.2 / 100.0
	VMI	1.0 / 2.8	8.4 / 20.9	99.7 / 100.0	0.2 / 0.4	5.2 / 15.0	98.2 / 100.0
	SSA	0.7 / 4.1	6.1 / 23.5	98.3 / 100.0	0.0 / 0.6	3.9 / 18.5	93.3 / 100.0
	DFANet	0.2 / 1.0	1.5 / 5.8	99.6 / 100.0	0.0 / 0.2	1.1 / 7.7	99.1 / 100.0
	SIA	1.0 / 5.9	10.6 / 36.6	98.4 / 100.0	0.1 / 2.4	9.0 / 24.4	96.3 / 100.0
	BSR	0.4 / 1.5	3.7 / 14.7	84.9 / 100.0	0.1 / 0.6	2.9 / 12.6	77.6 / 100.0
	BPFA	0.9 / 4.1	4.6 / 20.4	97.7 / 100.0	0.0 / 2.3	4.0 / 20.4	96.2 / 100.0

Face Recognition Models. The normal trained FR models employed in our experiments include IR152, FaceNet, and MobileFace (abbreviated as MF). These FR models are identical to those used in previous studies (Yin et al., 2021), (Hu et al., 2022), (Zhou et al., 2023b), and (Zhou et al., 2023a). Additionally, we incorporate adversarial robust FR models in our experiments, denoted as $IR152^{adv}$, $FaceNet^{adv}$, and MF^{adv} , which are identical to those used in (Zhou et al., 2023b).

For calculating the attack success rate in impersonation and dodging attacks, we choose the thresholds based on FAR@0.001 on the entire LFW dataset.

Attack Setting. Without any particular emphasis, we set the maximum allowable perturbation magnitude, denoted as ϵ , to 10. This value is based on the L_∞ norm bound, considering pixel values within the range of [0, 255]. Furthermore, we specify the maximum number of iterative steps as 200. Moreover, both β and γ are set to 1.0.

Evaluation Metrics. We employ the *attack success rate* (ASR) to assess the performance of various attacks. ASR represents the ratio of successfully attacked adversarial face examples.

Baseline methods Our proposed attack is a restricted attack method that aims to enhance the robustness of FR models. It is not rational to compare our proposed method with the

Table 2. Comparisons of dodging ASR with multi-task attacks on the LFW dataset. The models in the first row are the victim models.

	ASR ^d			ASR ⁱ
	IR152	FaceNet	MF	
Lagrangian	3.9	26.5	100.0	26.0
Lagrangian + ours	7.3	36.4	100.0	26.6
DA	11.0	35.6	99.1	37.4
DA + ours	17.5	44.9	99.4	37.8

unrestricted attacks which do not limit the magnitude of the adversarial perturbations. Therefore, we choose restricted attacks on FR that aim to enhance the robustness of FR models (Zhong & Deng, 2021) (Zhou et al., 2023b) and transfer attacks (Xie et al., 2019) (Long et al., 2022) (Wang et al., 2023b) (Wang et al., 2023a) as our baseline.

4.2. The Trade-off Between the Impersonation Attacks and Dodging Attacks

Owing to the inherent conflict during the optimization process of impersonation and dodging losses, there exists a trade-off between impersonation and dodging performance. We craft adversarial face examples using Lagrangian attack and our proposed PPR on LFW based on DI. The average black-box results are demonstrated in Figure 2.

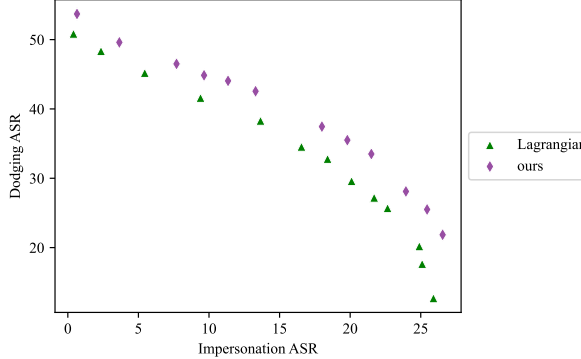


Figure 2. The trade-off between the performance of impersonation attack and dodging attack of adversarial examples.

Figure 2 illustrates that the inclusion of our proposed method into the Lagrangian attack results in reduced the trade-off. It is not hard to see the reason. The pruning operation of our proposed PPR serves to sparsify the adversarial perturbations while preserving the impersonation performance. On the other hand, the restoration operation tends to introduce adversarial perturbations in the pruned areas, specifically favoring dodging attacks. These operations effectively enhance the dodging attack performance while maintaining the impersonation attack performance, ultimately mitigating the trade-off.

4.3. Comparison Study

We compare our proposed attack method with the baseline attacks on multiple FR models and datasets. For our proposed method, we choose the Lagrangian attack as the attack for both the stages of pre-training and restoration. The results are shown in Table 1. The numbers before the slash represent the results of the baseline attack, which refers to the attack method mentioned in the seconds column that solely utilizes the traditional impersonation attacks to create the adversarial examples. On the other hand, the numbers after the slash correspond to the results obtained by combining the baseline attack with our proposed PPR.

Table 1 shows that after being added our proposed attack method, the dodging ASR of the adversarial attacks improve a lot. Note that the average black-box impersonation ASRs of the baseline attacks in Table 1 increase after incorporating our proposed attack method. This demonstrate the effectiveness of our proposed method in improving the dodging attack performance while maintain the impersonation attack performance.

Furthermore, we conducted a comparison between our proposed PPR and multi-task attacks using MF as the surrogate model on LFW. For our proposed method, we choose the

Table 3. Comparisons of dodging ASR on LFW with adversarial robust models as victim models.

Attack	ASR ^d			ASR ⁱ
	IR152 ^{adv}	FaceNet ^{adv}	MF ^{adv}	
DI	2.3	7.8	0.5	19.8
DI + ours	7.2	17.1	4.7	20.3
VMI	0.8	4.5	0.3	15.8
VMI + ours	3.3	8.9	3.0	16.2
SSA	0.6	2.9	0.1	14.7
SSA + ours	3.9	9.7	3.0	14.8
DFANet	0.2	0.8	0	8.1
DFANet + ours	0.3	1.3	0.1	8.3
SIA	1.4	6	0.2	17.5
SIA + ours	5.6	15.5	5.6	17.6
BSR	0.4	1.9	0	6.4
BSR + ours	0.7	3.5	0.4	6.6
BPFA	0.3	1.8	0.1	13.1
BPFA + ours	4.1	8.4	4.2	13.4

corresponding multi-task attack as the attack for both the stage of pre-training and restoration. The dodging attack ASR (denoted as ASR^d) and average black-box impersonation ASR (denoted as ASRⁱ) results are shown in Table 2. The numbers before the slash represent the results of the baseline multi-task attack, while the numbers after the slash indicate the results after integrating our proposed method into the baseline multi-task attack. It is noteworthy that the average black-box impersonation performance of our proposed attack surpasses that of the corresponding baseline multi-task attack. These results underscore the effectiveness of our method in enhancing the dodging performance of multi-task attacks while maintaining the impersonation performance.

In practical application scenarios, victims can employ adversarial robust models to defend against adversarial attacks. Consequently, it becomes crucial to evaluate the performance of adversarial attacks on these robust models. In this study, we generate adversarial examples on the LFW dataset using MF as the surrogate model and assess the performance of various attacks on the adversarial robust models. The results are presented in Table 3.

Table 3 illustrates that the inclusion of our proposed method leads to improvements in both dodging and impersonation performance. These results serve as evidence of the effectiveness of our proposed method on adversarial robust models.

4.4. Ablation Study

To delve deeper into the properties of our proposed attack method, we conducted an ablation experiment using DI as the Baseline attack, with MF serving as the surrogate model on the LFW dataset. To confirm the effectiveness of our pruning method, we employed the Random Zeroing (RZ) method, which randomly sets adversarial perturbations

Table 4. Comparisons of ASR results of dodging attack and impersonation attacks on the LFW dataset. * denote the method that only use the impersonation loss to craft the adversarial face examples.

	ASR ^d			ASR ⁱ
	IR152	FaceNet	MF	
Baseline	2.2	18.2	99.2	25.6
Lagrangian	3.9	26.5	100.0	26.0
<i>Fine-tuning</i>	3.4	23.2	99.9	25.8
<i>RZ</i>	0.6	4.4	94.8	15.1
<i>Pruning</i>	3.4	24.8	100.0	25.4
PPR	6.8	35.5	100.0	25.9

to zero. We applied this method and our pruning method to free up 20% of the adversarial perturbations. For *Fine-tuning*, we employed the Lagrangian attack as the method to further optimize the adversarial examples crafted by the Lagrangian attack. The dodging attack ASR and average black-box impersonation ASR results are shown in Table 4.

Table 4 demonstrates that our proposed pruning method for adversarial examples achieves a significantly smaller decrease in ASR than *RZ* after pruning 20% of adversarial perturbations, indicating the effectiveness of our proposed approach. After pruning and restoration, adversarial perturbations using our proposed *Pruning* method, both impersonation and dodging ASR of the crafted adversarial face examples are recovered and higher than the Baseline attack method. These results demonstrate the effectiveness of our proposed PPR in improving the dodging performance of adversarial attacks on FR without compromising the impersonation attack performance.

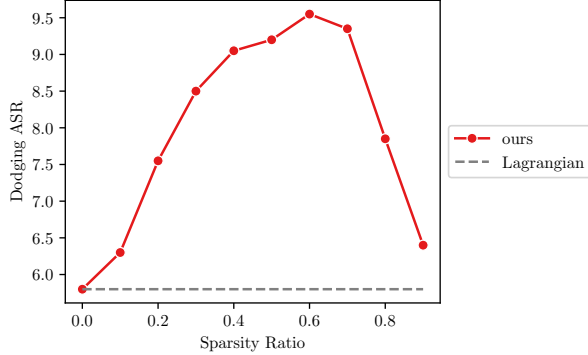


Figure 3. The dodging ASR in different sparsity ratio.

4.5. Hyperparameter Sensitivity Study

The sparsity ratio quantifies the proportion of adversarial perturbations that are allowed to be discarded during the

pruning stage. This ratio greatly impacts the performance of our proposed attack method. Hence, we conducted a sensitivity study on the sparsity ratio to analyze its effect on performance of the algorithm. We selected the DI-based Lagrangian attack method as the Baseline for pre-training and performed a hyperparameter sensitivity study on LFW with FaceNet as the surrogate model. We adjusted the value of λ to ensure that the average black-box impersonation ASR results were within a 0.8% absolute difference compared to the corresponding Baseline. The dodging ASR results are illustrated in Figure 3.

Figure 3 illustrates that the dodging ASR of our proposed method initially increases and then decreases as the sparsity ratio increases. It is not hard to see the reason; When the sparsity ratio increases, a greater number of adversarial perturbations are pruned, creating more empty regions for the adversarial perturbations that favor dodging attacks in the restoration stage. If the sparsity ratio is set to a too high value, an excessive number of adversarial perturbations are allowed to be freed up, resulting in a degradation of performance for the pre-trained adversarial examples. Consequently, the performance of adversarial face examples will decrease.

5. Conclusion

In this paper, we delve into the issue of multi-identity samples present among adversarial face examples. Our research reveals that traditional impersonation attacks often involve multi-identity samples and the success of a traditional impersonation attack may not necessarily imply success in dodging attacks in the black-box setting. In order to improve dodging performance without compromising impersonation performance, we proposed a novel attack known as PPR. PPR involves pruning the adversarial examples to release some of the adversarial perturbations while tending to maintain the performance of the adversarial examples. We then restore the adversarial perturbation in the pruned area, which favors dodging attack, to enhance the performance of dodging attack without harming the performance of the impersonation attack. Our extensive experiments demonstrate the effectiveness of our proposed attack method.

6. Potential Broader Impact

This paper showcases research dedicated to advancing the field of Machine Learning. The proposed attack method could jeopardize the security of FR systems. Our aim is to raise awareness through our proposed attack method and reinforce the robustness of FR systems.

References

Borgwardt, K. M., Gretton, A., Rasch, M. J., Kriegel, H., Schölkopf, B., and Smola, A. J. Integrating structured biological data by kernel maximum mean discrepancy. In *Proceedings 14th International Conference on Intelligent Systems for Molecular Biology*, pp. 49–57, 2006.

Cao, X. and Gong, N. Z. Mitigating evasion attacks to deep neural networks via region-based classification. *Proceedings of the 33rd Annual Computer Security Applications Conference*, 2017.

Cherepanova, V., Goldblum, M., Foley, H., Duan, S., Dickerson, J. P., Taylor, G., and Goldstein, T. Lowkey: Leveraging adversarial attacks to protect social media users from facial recognition. In *International Conference on Learning Representations*, 2021.

Deng, J., Guo, J., Yang, J., Xue, N., Kotsia, I., and Zafeiriou, S. Arcface: Additive angular margin loss for deep face recognition. *IEEE Transactions on Pattern Analysis and Machine Intelligence*, 44(10):5962–5979, 2022. doi: 10.1109/TPAMI.2021.3087709.

Frantar, E. and Alistarh, D. Sparsegpt: Massive language models can be accurately pruned in one-shot. *ArXiv*, abs/2301.00774, 2023.

Goodfellow, I. J., Shlens, J., and Szegedy, C. Explaining and harnessing adversarial examples. In *International Conference on Learning Representations*, 2015.

Hu, S., Liu, X., Zhang, Y., Li, M., Zhang, L. Y., Jin, H., and Wu, L. Protecting facial privacy: Generating adversarial identity masks via style-robust makeup transfer. In *Proceedings of the IEEE conference on computer vision and pattern recognition*, pp. 14994–15003, 2022.

Huang, G. B., Ramesh, M., Berg, T., and Learned-Miller, E. Labeled faces in the wild: A database for studying face recognition in unconstrained environments. Technical Report 07-49, University of Massachusetts, Amherst, October 2007.

Huang, Y., Shen, P., Tai, Y., Li, S., Liu, X., Li, J., Huang, F., and Ji, R. Improving face recognition from hard samples via distribution distillation loss. In *European Conference on Computer Vision*, 2020.

Jia, S., Yin, B., Yao, T., Ding, S., Shen, C., Yang, X., and Ma, C. Adv-attribute: Inconspicuous and transferable adversarial attack on face recognition. In *NeurIPS*, 2022. URL http://papers.nips.cc/paper_files/paper/2022/hash/dccbeb7a8df3065c4646928985edf435-Abstract.html.

Karras, T., Aila, T., Laine, S., and Lehtinen, J. Progressive growing of gans for improved quality, stability, and variation. In *International Conference on Learning Representation*, 2018.

Li, Y., Li, Y., Dai, X., Guo, S., and Xiao, B. Physical-world optical adversarial attacks on 3d face recognition. In *IEEE/CVF Conference on Computer Vision and Pattern Recognition, CVPR 2023, Vancouver, BC, Canada, June 17–24, 2023*, pp. 24699–24708. IEEE, 2023a. doi: 10.1109/CVPR52729.2023.02366. URL <https://doi.org/10.1109/CVPR52729.2023.02366>.

Li, Y., Li, Y., Dai, X., Guo, S., and Xiao, B. Physical-world optical adversarial attacks on 3d face recognition. In *2023 IEEE/CVF Conference on Computer Vision and Pattern Recognition (CVPR)*, pp. 24699–24708, 2023b. doi: 10.1109/CVPR52729.2023.02366.

Liang, C., Wu, X., Hua, Y., Zhang, J., Xue, Y., Song, T., Xue, Z., Ma, R., and Guan, H. Adversarial example does good: Preventing painting imitation from diffusion models via adversarial examples. In *International Conference on Machine Learning*, pp. 20763–20786. PMLR, 2023.

Long, Y., Zhang, Q., Zeng, B., Gao, L., Liu, X., Zhang, J., and Song, J. Frequency domain model augmentation for adversarial attack. In *European conference on computer vision*, volume 13664, pp. 549–566, 2022.

Lu, D., Wang, Z., Wang, T., Guan, W., Gao, H., and Zheng, F. Set-level guidance attack: Boosting adversarial transferability of vision-language pre-training models. In *Proceedings of the IEEE/CVF International Conference on Computer Vision*, pp. 102–111, 2023.

Ma, X., Fang, G., and Wang, X. Llm-pruner: On the structural pruning of large language models. *ArXiv*, abs/2305.11627, 2023.

Naseer, M., Mahmood, A., Khan, S., and Khan, F. Boosting adversarial transferability using dynamic cues. In *International Conference on Learning Representation*, 2023.

Qiu, H., Xiao, C., Yang, L., Yan, X., Lee, H., and Li, B. Semanticadv: Generating adversarial examples via attribute-conditioned image editing. In *Computer Vision–ECCV 2020: 16th European Conference, Glasgow, UK, August 23–28, 2020, Proceedings, Part XIV 16*, pp. 19–37. Springer, 2020.

Schroff, F., Kalenichenko, D., and Philbin, J. Facenet: A unified embedding for face recognition and clustering. In *Proceedings of the IEEE Conference on Computer Vision and Pattern Recognition*, pp. 815–823, 2015.

Shamshad, F., Naseer, M., and Nandakumar, K. Clip2protect: Protecting facial privacy using text-guided makeup via adversarial latent search. In *Proceedings of the IEEE/CVF Conference on Computer Vision and Pattern Recognition*, pp. 20595–20605, 2023.

Szegedy, C., Zaremba, W., Sutskever, I., Bruna, J., Erhan, D., Goodfellow, I. J., and Fergus, R. Intriguing properties of neural networks. In Bengio, Y. and LeCun, Y. (eds.), *2nd International Conference on Learning Representations, ICLR 2014, Banff, AB, Canada, April 14–16, 2014, Conference Track Proceedings*, 2014. URL <http://arxiv.org/abs/1312.6199>.

Wang, H., Wang, Y., Zhou, Z., Ji, X., Gong, D., Zhou, J., Li, Z., and Liu, W. Cosface: Large margin cosine loss for deep face recognition. In *IEEE/CVF Conference on Computer Vision and Pattern Recognition*, 2018.

Wang, K., He, X., Wang, W., and Wang, X. Boosting adversarial transferability by block shuffle and rotation. *arXiv preprint arXiv:2308.10299*, 2023a.

Wang, X. and He, K. Enhancing the transferability of adversarial attacks through variance tuning. In *Proceedings of the IEEE Conference on Computer Vision and Pattern Recognition*, pp. 1924–1933, 2021.

Wang, X., Zhang, Z., and Zhang, J. Structure invariant transformation for better adversarial transferability. In *Proceedings of the IEEE/CVF International Conference on Computer Vision*, pp. 4607–4619, 2023b.

Wei, X., Huang, Y., Sun, Y., and Yu, J. Unified adversarial patch for cross-modal attacks in the physical world. In *Proceedings of the IEEE/CVF International Conference on Computer Vision*, pp. 4445–4454, 2023.

Wen, S. and Itti, L. Beneficial perturbations network for defending adversarial examples. *arXiv preprint arXiv:2009.12724*. URL <http://arxiv.org/abs/2009.12724>.

Xiao, Z., Gao, X., Fu, C., Dong, Y., Gao, W., Zhang, X., Zhou, J., and Zhu, J. Improving transferability of adversarial patches on face recognition with generative models. In *Proceedings of the IEEE conference on computer vision and pattern recognition*, pp. 11840–11849, 2021.

Xie, C., Zhang, Z., Zhou, Y., Bai, S., Wang, J., Ren, Z., and Yuille, A. L. Improving transferability of adversarial examples with input diversity. In *Proceedings of the IEEE Conference on Computer Vision and Pattern Recognition*, pp. 2730–2739, 2019.

Yang, X., Dong, Y., Pang, T., Su, H., Zhu, J., Chen, Y., and Xue, H. Towards face encryption by generating adversarial identity masks. In *Proceedings of the IEEE International Conference on Computer Vision*, pp. 3877–3887, 2021.

Yang, X., Liu, C., Xu, L., Wang, Y., Dong, Y., Chen, N., Su, H., and Zhu, J. Towards effective adversarial textured 3d meshes on physical face recognition. In *2023 IEEE/CVF Conference on Computer Vision and Pattern Recognition (CVPR)*, pp. 4119–4128, 2023. doi: 10.1109/CVPR52729.2023.00401.

Yin, B., Wang, W., Yao, T., Guo, J., Kong, Z., Ding, S., Li, J., and Liu, C. Adv-makeup: A new imperceptible and transferable attack on face recognition. In *International Joint Conference on Artificial Intelligence*, pp. 1252–1258, 2021.

Yuan, Z., Zhang, J., and Shan, S. Adaptive image transformations for transfer-based adversarial attack. In Avidan, S., Brostow, G. J., Cissé, M., Farinella, G. M., and Hassner, T. (eds.), *European Conference on Computer Vision*, pp. 1–17, 2022.

Zeng, D., Shi, H., Du, H., Wang, J., Lei, Z., and Mei, T. Npcface: Negative-positive collaborative training for large-scale face recognition. 2020.

Zhang, J., Wu, W., Huang, J., Huang, Y., Wang, W., Su, Y., and Lyu, M. R. Improving adversarial transferability via neuron attribution-based attacks. In *Proceedings of the IEEE conference on computer vision and pattern recognition*, pp. 14973–14982, 2022.

Zhong, Y. and Deng, W. Adversarial learning with margin-based triplet embedding regularization. In *Proceedings of the IEEE International Conference on Computer Vision*, pp. 6548–6557, 2019.

Zhong, Y. and Deng, W. Towards transferable adversarial attack against deep face recognition. *IEEE Transactions on Information Forensics and Security*, 16:1452–1466, 2021.

Zhou, F., Ling, H., Shi, Y., Chen, J., and Li, P. Improving visual quality and transferability of adversarial attacks on face recognition simultaneously with adversarial restoration, 2023a.

Zhou, F., Ling, H., Shi, Y., Chen, J., Li, Z., and Li, P. Improving the transferability of adversarial attacks on face recognition with beneficial perturbation feature augmentation. *IEEE Transactions on Computational Social Systems*, pp. 1–13, 2023b. doi: 10.1109/TCSS.2023.3291565.

A. Multi-identity Samples among the Benign Face Images

Multi-identity samples are intriguing samples that can be classified as multiple classes in FR. In this subsection, we will explore the existence of multi-identity samples among the benign face images (i.e. the face images without being added adversarial perturbations).

We randomly select negative face pairs from the entire LFW dataset. Subsequently, we use MF as our FR model to extract the embeddings of the face images in each face pair and calculate the cosine similarity between the two images. If the cosine similarity surpasses the threshold, both images in the pair are classified as belonging to multiple identities, indicating that they are multi-identity samples. Our findings demonstrate the presence of multi-identity samples among the benign face images, as illustrated in Figure 4.

Figure 4 illustrates that the multi-identity samples among the benign face images closely resemble the appearances of the identities they are classified into, suggesting they are hard samples (Zhou et al., 2023b) (Huang et al., 2020).

To analyze the cause of this phenomenon, we need to consider the properties of both the multi-identity samples and the FR model. Commonly-used FR models are well-trained and capable of correctly classifying the majority of benign face images. However, there are some benign face images that the FR model fails to classify accurately, and these samples are referred to as hard samples. Multi-identity samples are a specific type of hard sample known as hard negative samples. Typically, hard negative samples exhibit a similar appearance (Zeng et al., 2020), indicating that the multi-identity samples among the benign face images share a resemblance.

B. Universality of Multi-identity Samples among Adversarial Face Examples

The traditional impersonation attacks craft adversarial face example only use the impersonation loss (e.g. Equation (5)). In this subsection, we will investigate the ratio of multi-identity samples and evaluate the effectiveness of traditional impersonation attacks in terms of dodging attacks. We utilize the multi-identity sample ratio (MSR) to gauge the proportion of multi-identity samples that can be recognized as both the attacker and victim identities in the adversarial face examples capable of executing successful impersonation attacks. MSR be calculate as:

$$\text{MSR} = \frac{|\mathcal{S}_1 \cap \mathcal{S}_2|}{|\mathcal{S}_2|} \quad (18)$$

where \mathcal{S}_1 and \mathcal{S}_2 are the set of the adversarial examples that are identified as the attacker and victim identities, respectively. Therefore, the \mathcal{S}_2 is the set of the adversarial face



Figure 4. The Illustration of the multi-identity samples. The images in the first row and third row are the images of different identities. The image in the second row are the images of the multi-identities samples that will be recognized as the identities both top and below it by the FR model.

examples that can perform successful impersonation attack. Equation (3) can be rewritten as:

$$\text{ASR}^i = \frac{|\mathcal{S}_2|}{N_p} \quad (19)$$

We evaluate the MSR, impersonation attack ASR and dodging attack ASR using MF as the surrogate model on the LFW dataset. The results are shown in Table 5.

Table 5 demonstrate that most of the crafted adversarial face examples are multi-identity samples when the victim model are the black-box model. This indicates that most adversarial face examples generated through traditional impersonation attacks are unable to attain a successful dodging attack in the black-box setting. Nevertheless, in the white-box setting, the majority of adversarial face examples capable of executing successful impersonation attacks also demonstrate success in dodging attacks.

To analyze the reason, we need to consider the metric used to determine whether two face images belong to the same identity in FR. FR is an open-set task, so we utilize the distance in the embedding space to make this determination. Figure 5 illustrates two decision boundaries for each FR model, one for attacker identity and one for victim identity.

In the white-box setting, if we generate adversarial examples using Equation (5), these examples can enter a space in which they are identified as the victim identity but not as the attacker identity. However, the decision boundary of the black-box model differs from that of the surrogate model. In the black-box setting, most adversarial examples are found

Table 5. The results (%) on the LFW dataset. The models on the first row are the victim models.

Attack	Metric	IR152	FaceNet	MF
DI	MSR	95.6	75.7	0.8
	ASR ⁱ	18.4	32.9	100.0
	ASR ^d	2.2	18.2	99.2
VMI	MSR	97.0	88.6	0.3
	ASR ⁱ	13.6	20.2	100.0
	ASR ^d	1.0	8.4	99.7
SSA	MSR	98.6	92.8	1.5
	ASR ⁱ	13.8	19.6	100.0
	ASR ^d	0.7	5.9	98.5
DFANet	MSR	98.6	96.6	0.4
	ASR ⁱ	7.0	11.9	100.0
	ASR ^d	0.2	1.5	99.6
SIA	MSR	97.4	83.9	1.6
	ASR ⁱ	15.7	26.7	100.0
	ASR ^d	1.0	10.6	98.4
BSR	MSR	98.1	96.8	15.1
	ASR ⁱ	5.4	9.5	100.0
	ASR ^d	0.4	3.7	84.9
BPFA	MSR	96.2	92.1	2.3
	ASR ⁱ	15.8	17.8	100
	ASR ^d	0.9	4.6	97.7

between the decision boundaries of the black-box model, resulting in the majority of adversarial examples crafted using Equation (5) being multi-identity samples. This demonstrates that the adversarial face examples are positioned near the decision boundary, aligning with findings from prior research of adversarial attacks on image classification (Cao & Gong, 2017).

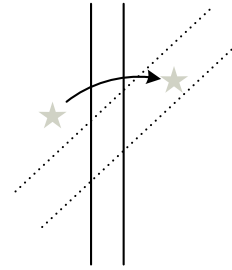


Figure 5. Illustration of the decision boundaries of FR models. The star in the left and right are the initial image of the adversarial face examples (i.e. the attacker image) and the final adversarial example, respectively. The solid and dashed lines are the decision boundaries for the surrogate and black-box models, respectively. For both the surrogate and black-box models, the lines in the left and right are the decision boundary of the victim and attacker, respectively.